JACS
JOURNAL OF THE AMERICAN CHEMICAL SOCIETY

Subscriber access provided by American Chemical Society

Article

Carbon–Fluorine Bond Activation Coupled with Carbon–Hydrogen Bond Formation to Iridium: Kinetics, Mechanism, and Diastereoselectivity

Shaun A. Garratt, Russell P. Hughes, Ivan Kovacik, Antony J. Ward, Stefan Willemsen, and Donghui Zhang

J. Am. Chem. Soc., **2005**, 127 (44), 15585-15594• DOI: 10.1021/ja0545012 • Publication Date (Web): 06 October 2005

Downloaded from http://pubs.acs.org on March 25, 2009

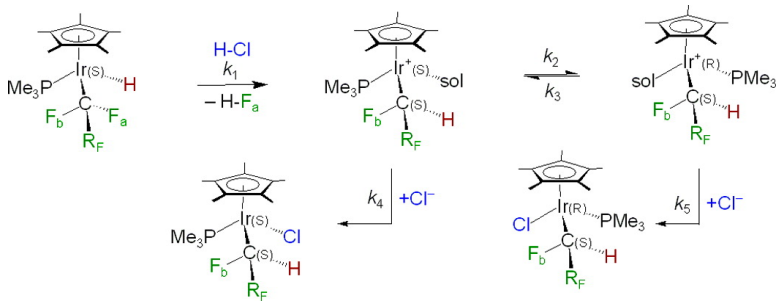

More About This Article

Additional resources and features associated with this article are available within the HTML version:

- Supporting Information
- Links to the 4 articles that cite this article, as of the time of this article download
- Access to high resolution figures
- Links to articles and content related to this article
- Copyright permission to reproduce figures and/or text from this article

View the Full Text HTML

ACS Publications
High quality. High impact.

Journal of the American Chemical Society is published by the American Chemical Society. 1155 Sixteenth Street N.W., Washington, DC 20036

J|A|C|S
ARTICLES
Published on Web 10/06/2005

Carbon−Fluorine Bond Activation Coupled with Carbon−Hydrogen Bond Formation α to Iridium: Kinetics, Mechanism, and Diastereoselectivity

Shaun A. Garratt, Russell P. Hughes,* Ivan Kovacik, Antony J. Ward, Stefan Willemsen, and Donghui Zhang

Contribution from the Department of Chemistry, 6128 Burke Laboratory, Dartmouth College, Hanover, New Hampshire 03755

Received July 7, 2005; E-mail: rph@dartmouth.edu

Abstract: Reactions of iridium(fluoroalkyl)hydride complexes $Cp^*Ir(PMe_3)(CF_2R_F)Y$ (R_F = F, CF_3; Y = H, D) with LutHX (Lut = 2,6-dimethylpyridine; X = Cl, I) results in C−F activation coupled with hydride migration to give $Cp^*Ir(PMe_3)(CYFR_F)X$ as variable mixtures of diastereomers. Solution conformations and relative diastereomer configurations of the products have been determined by $^{19}F\{^1H\}$HOESY NMR to be (S_C, S_{Ir})(R_C, R_{Ir}) for the kinetic diastereomer and (R_C, S_{Ir})(S_C, R_{Ir}) for its thermodynamic counterpart. Isotope labeling experiments using LutDCl/$Cp^*Ir(PMe_3)(CF_2R_F)$H and $Cp^*Ir(PMe_3)(CF_2R_F)$D/LutHCl showed that, unlike a previously studied system, H/D exchange is faster than protonation of the α-CF bond, giving an identical mixture of product isotopologues from both reaction mixtures. The kinetic rate law shows a first-order dependence on the concentration of iridium substrate, but a half-order dependence on that of LutHCl; this is interpreted to mean that LutHCl dissociates to give HCl as the active protic source for C−F bond activation. Detailed kinetic studies are reported, which demonstrate that lack of complete diastereoselectivity is not a function of the C−F bond activation/H migration steps but that a cationic intermediate plays a double role in loss of diastereoselectivity; the intermediate can undergo epimerization at iridium before being trapped by halide and can also catalyze the epimerization of kinetic diastereomer product to thermodynamic product. A detailed mechanism is proposed and simulations performed to fit the kinetic data.

Introduction

There is a significant effort in the organometallic community to find ways of functionalizing normally unreactive and strong bonds such as those between carbon and hydrogen, or carbon and fluorine. In some ways the latter task is especially challenging due to the strength of the C−F bond, the strongest single bond to carbon,[1] and has been the subject of much study, both experimental and computational.[2−27] The synthesis of fluorinated stereocenters can also be challenging.[28] While some naturally occurring molecules contain such chiral centers,[29] the traditional method of synthesis has been to form a new C−F bond selectively using a fluorinating reagent, typically contain-

(1) Smart, B. E. Fluorocarbons. In *Chemistry of Functional Groups, Supplement D*; Patai, S., Rappoport, Z., Eds.; Wiley: New York, 1983; Chapter 14, pp 603−655.
(2) Hughes, R. P.; Laritchev, R. B.; Zakharov, L. N.; Rheingold, A. L. *J. Am. Chem. Soc.* **2004**, *126*, 2308−2309.
(3) Reinhold, M.; McGrady, J. E.; Perutz, R. N. *J. Am. Chem. Soc.* **2004**, *126*, 5268−5276.
(4) Clot, E.; Mégret, C.; Kraft, B. M.; Eisenstein, O.; Jones, W. D. *J. Am. Chem. Soc.* **2004**, *126*, 5647−5653.
(5) Noveski, D.; Braun, T.; Schulte, M.; Neumann, B.; Stammler, H.-G. *J. Chem. Soc., Dalton Trans.* **2003**, 4075−4083.
(6) Jones, W. D. *J. Chem. Soc., Dalton Trans.* **2003**, 3991−3995.
(7) Braun, T.; Perutz, R. N. *Chem. Commun.* **2002**, 2749−2757.
(8) Braun, T.; Noveski, D.; Neumann, B.; Stammler, H.-G. *Angew. Chem., Int. Ed.* **2002**, *41*, 2745−2748.
(9) Braun, T.; Perutz, R. N.; Sladek, M. I. *Chem. Commun.* **2001**, 2254−2255.
(10) Braun, T.; Cronin, L.; Higgitt, C. L.; McGrady, J. E.; Perutz, R. N.; Reinhold, M. *New. J. Chem.* **2001**, *25*, 19−21.
(11) McAlexander, L. H.; Beck, C. M.; Burdeniuc, J. J.; Crabtree, R. H. *J. Fluorine Chem.* **1999**, *99*, 67−72.
(12) Braun, T.; Foxon, S. P.; Perutz, R. N.; Walton, P. H. *Angew. Chem., Int. Ed.* **1999**, *38*, 3326−3329.
(13) Whittlesey, M. K.; Perutz, R. N.; Greener, B.; Moore, M. H. *Chem. Commun.* **1997**, 187−188.
(14) Edelbach, B. L.; Jones, W. D. *J. Am. Chem. Soc.* **1997**, *119*, 7734−7742.
(15) Cronin, L.; Higgitt, C. L.; Karch, R.; Perutz, R. N. *Organometallics* **1997**, *16*, 4920−4928.
(16) Burdeniuc, J.; Jedlicka, B.; Crabtree, R. H. *Chem. Ber./Recl.* **1997**, *130*, 145−154.
(17) Whittlesey, M. K.; Perutz, R. N.; Moore, M. H. *Chem. Commun.* **1996**, 787−788.
(18) Kiplinger, J. L.; Richmond, T. G. *J. Am. Chem. Soc.* **1996**, *118*, 1805−1806.
(19) Kiplinger, J. L.; Richmond, T. G. *Chem. Commun.* **1996**, 1115−1116.
(20) Kiplinger, J. L.; Richmond, T. G.; Osterberg, C. E. *Chem. Rev.* **1994**, *94*, 373−431.
(21) Aizenberg, M.; Milstein, D. *Science* **1994**, *265*, 359−361.
(22) Weydert, M.; Andersen, R. A.; Bergman, R. G. *J. Am. Chem. Soc.* **1993**, *115*, 8837−8838.
(23) Belt, S. T.; Helliwell, M.; Jones, W. D.; Partridge, M. G.; Perutz, R. N. *J. Am. Chem. Soc.* **1993**, *115*, 1429−1440.
(24) Klahn, A. H.; Moore, M. H.; Perutz, R. N. *J. Chem. Soc., Chem. Commun.* **1992**, 1699−1701.
(25) Jones, W. D.; Partridge, M. G.; Perutz, R. N. *J. Chem. Soc., Chem. Commun.* **1991**, 264−266.
(26) Jones, M. T.; McDonald, R. N. *Organometallics* **1988**, *5*, 1221−1223.
(27) Mazurek, U.; Schwarz, H. *Chem. Commun.* **2003**, 1321−1326.
(28) Ramachandran, P. V., Ed.; *Asymmetric Fluoroorganic Chemistry*; *Synthesis, Applications, and Future Directions*; ACS Symposium Series 746; American Chemical Society: Washington, DC, 2000.
(29) Filler, R. In *Fluorine-Containing Chiral Compounds of Biomedical Interest*; Ramachandran, P. V., Ed.; ACS Symposium Series 746; American Chemical Society: Washington, DC, 2001; pp 1−20.

Scheme 1

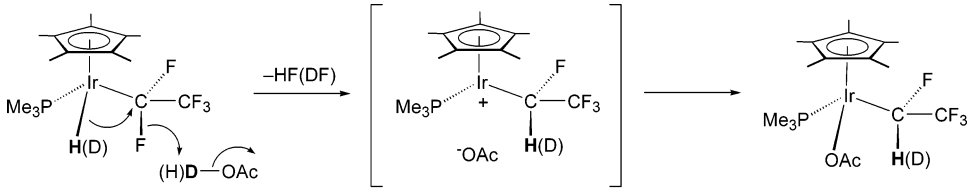

1a R = H
1b R = D

2a R = H
2b R = D

ing a metal.[30−39] A complementary approach to fluorinated stereocenters would be to *break* a C−F bond in a selective manner to give the stereocenter, clearly a more difficult thermodynamic process due to the strength of the C−F bond.[1] However, it is now apparent that aliphatic C−F bonds α to certain transition metal centers are activated toward attack by exogenous protic[40−43] or Lewis acids,[44−48] with a strong bond to H or a main group element providing significant thermodynamic compensation for breaking the C−F bond. In some cases, this process occurs in combination with hydride migration from metal to the α-C,[49−51] providing some encouragement that selective C−F bond activation could be realized.

Following our initial discovery that cationic iridium−fluoroalkyl compounds react with elemental dihydrogen to give free hydrofluorocarbons (HFCs),[52] we demonstrated that this process involved a heterolytic activation of H_2 to give an iridium hydride and an exogenous proton. Subsequent C−F bond activation by the exogenous proton afforded defluorination and accompanying hydride migration to carbon. Specifically, treatment of the independently prepared hydride complex Cp*Ir(PMe_3)(CF_2CF_3)H (**1a**)[53] with CH_3CO_2H in CD_2Cl_2 afforded two diastereomers of the acetate product in a 2:1 ratio as shown in Scheme 1.[54] When CH_3CO_2D was used, around 10% of Cp*Ir(PMe_3)(CDFCF$_3$)OAc (**2b**) was observed along with the protio analogue **2a**. This result was consistent with two competing processes; exogenous deuteronation at fluorine with intramolecular H migration to give the principal product and competitive scrambling of H^+ and D^+ (and thereby **1a** and **1b**) via a presumed η^2-HD intermediate. However, the fact that only a small amount of deuterium was found on the α-carbon in the product indicated that the dominant process was the former. This was confirmed by using the corresponding iridium-deuteride (**1b**) and CH_3CO_2H, in which **2b** was the dominant product, with some formation of **2a** occurring by H/D exchange. For each product isotopologue, the diastereoselectivity was about 2:1, and no significant kinetic isotope effects were observed.[54]

Although H(D)-migration showed some diastereoselectivity, we subsequently demonstrated that the reaction of Cp*Ir(PMe_3)($CF_2CF_2CF_3$)Me (**3**) with the weakly acidic 2,6-lutidinium chloride (LutHCl) proceeds quantitatively to give Cp*Ir(PMe_3)[CF(Me)CF_2CF_3]Cl (**4**) as a *single diastereomer*. The relative configurations of the Ir and C stereocenters in **4** were defined crystallographically as (R_{Ir}, R_C)(S_{Ir}, S_C).[55] No free methane formation was observed, and use of 2,6-lutidinium-(D)-chloride (LutDCl) gave no D-incorporation into the CF(Me)C_2F_5 group. This is consistent with external protonation occurring exclusively at the α-CF bond to the complete exclusion of protonation at the Ir−CH_3 bond to give the kind of η-methane intermediate found in many other systems.[56−66] Furthermore, in a recently published study of C−F bond activation coupled with vinyl migration, in which the intermediate is trapped by the pendant vinyl group before anion coordination, we have provided evidence that the *S*-enantiomer of the starting material affords the *S*-configuration at carbon in the product and that C−F bond activation is completely diastereoselective.[67] Observation of complete diastereoselectivity in these other migration reactions prompted a return look at the original hydride migration system in an attempt to address the reasons for the lower diastereoselectivity observed and to further clarify the overall mechanistic features of this reaction.

(30) Gouverneur, V.; Greedy, B. *Chem. Eur. J.* **2002**, *8*, 766−771.
(31) Mohar, B.; Baudoux, J.; Plaquevent, J.-C.; Cahard, D. *Angew. Chem., Int. Ed.* **2001**, *40*, 4214−4216.
(32) Piana, S.; Devillers, I.; Togni, A.; Rothlisberger, U. *Angew. Chem., Int. Ed.* **2002**, *41*, 979−982.
(33) Prakesch, M.; Grée, D.; Grée, R. *Acc. Chem. Res.* **2002**, *35*, 175−181.
(34) Muniz, K. *Angew. Chem., Int. Ed.* **2001**, *40*, 1653−1656.
(35) Shibata, N.; Liu, Z.; Takeuchi, Y. *Chem. Pharm. Bull.* **2000**, *48*, 1954−1958.
(36) Togni, A.; Mezzetti, A.; Barthazy, P.; Becker, C.; Devillers, I.; Frantz, R.; Hintermann, L.; Perseghini, M.; Sanna, M. *Chimia* **2001**, *55*, 801−805.
(37) Liu, Z.; Shibata, N.; Takeuchi, Y. *J. Org. Chem.* **2000**, *65*, 7583−7587.
(38) Differding, E.; Lang, R. W. *Tetrahedron Lett.* **1988**, *29*, 6087−6090.
(39) Iseki, K. *Tetrahedron* **1998**, *54*, 13887−13914.
(40) Appleton, T. G.; Berry, R. D.; Hall, J. R.; Neale, D. W. *J. Organomet. Chem.* **1989**, *364*, 249−273.
(41) Clark, G. R.; Hoskins, S. V.; Roper, W. R. *J. Organomet. Chem.* **1982**, *234*, C9−C12.
(42) Burrell, A. K.; Clark, G. R.; Rickard, C. E. F.; Roper, W. R. *J. Organomet. Chem.* **1994**, *482*, 261−269.
(43) Michelin, R. A.; Ros, R.; Guadalupi, G.; Bombieri, G.; Benetollo, F.; Chapuis, G. *Inorg. Chem.* **1989**, *28*, 840−846.
(44) Koola, J. D.; Roddick, D. M. *Organometallics* **1991**, *10*, 591−597.
(45) Crespi, A. M.; Shriver, D. F. *Organometallics* **1985**, *4*, 1830−1835.
(46) Richmond, T. G.; Shriver, D. F. *Organometallics* **1984**, *3*, 305−314.
(47) Richmond, T. G.; Crespi, A. M.; Shriver, D. F. *Organometallics* **1984**, *3*, 314−319.
(48) Reger, D. L.; Dukes, M. D. *J. Organomet. Chem.* **1978**, *153*, 67−72.
(49) Huang, D.; Caulton, K. G. *J. Am. Chem. Soc.* **1997**, *119*, 3185−3186.
(50) Greene, T. R.; Roper, W. R. *J. Organomet. Chem.* **1986**, *299*, 245−250.
(51) Burrell, A. K.; Clark, G. R.; Jeffrey, J. G.; Rickard, C. E. F.; Roper, W. R. *J. Organomet. Chem.* **1990**, *388*, 391−408.
(52) Hughes, R. P.; Smith, J. M. *J. Am. Chem. Soc.* **1999**, *121*, 6084−6085.
(53) Hughes, R. P.; Kovacik, I.; Lindner, D. C.; Smith, J. M.; Willemsen, S.; Zhang, D.; Guzei, I. A.; Rheingold, A. L. *Organometallics* **2001**, *20*, 3190−3197.
(54) Hughes, R. P.; Willemsen, S.; Williamson, A.; Zhang, D. *Organometallics* **2002**, *21*, 3085−3087.
(55) Hughes, R. P.; Zhang, D.; Zakharov, L. N.; Rheingold, A. L. *Organometallics* **2002**, *21*, 4902−4904.
(56) Bullock, R. M.; Headford, C. E. L.; Hennessy, K. M.; Kegley, S. E.; Norton, J. R. *J. Am. Chem. Soc.* **1989**, *111*, 3897−3908.
(57) Johansson, L.; Tilset, M. *J. Am. Chem. Soc.* **2001**, *123*, 739−740.
(58) Wik, B. J.; Lersch, M.; Tilset, M. *J. Am. Chem. Soc.* **2002**, *124*, 12116−12117.
(59) Jones, W. D. *Acc. Chem. Res.* **2003**, *36*, 140−146.
(60) Hall, C.; Perutz, R. N. *Chem. Rev.* **1996**, *96*, 3125−3146.
(61) Gross, C. L.; Girolami, G. S. *J. Am. Chem. Soc.* **1998**, *120*, 6605−6606.
(62) Northcutt, T. O.; Wick, D. D.; Vetter, A. J.; Jones, W. D. *J. Am. Chem. Soc.* **2001**, *123*, 7257−7270.
(63) Stahl, S.; Labinger, J. A.; Bercaw, J. E. *Angew. Chem., Int. Ed.* **1998**, *37*, 2181−2192.
(64) Stahl, S. S.; Labinger, J. A.; Bercaw, J. E. *J. Am. Chem. Soc.* **1995**, *117*, 9371−9372.
(65) Stahl, S. S.; Labinger, J. A.; Bercaw, J. E. *J. Am. Chem. Soc.* **1996**, *118*, 5961−5976.
(66) Labinger, J. A.; Bercaw, J. E. *Nature* **2002**, *417*, 507−514.
(67) Hughes, R. P.; Laritchev, R. B.; Zakharov, L. N.; Rheingold, A. L. *J. Am. Chem. Soc.* **2005**, *127*, 6325−6334.

Scheme 2

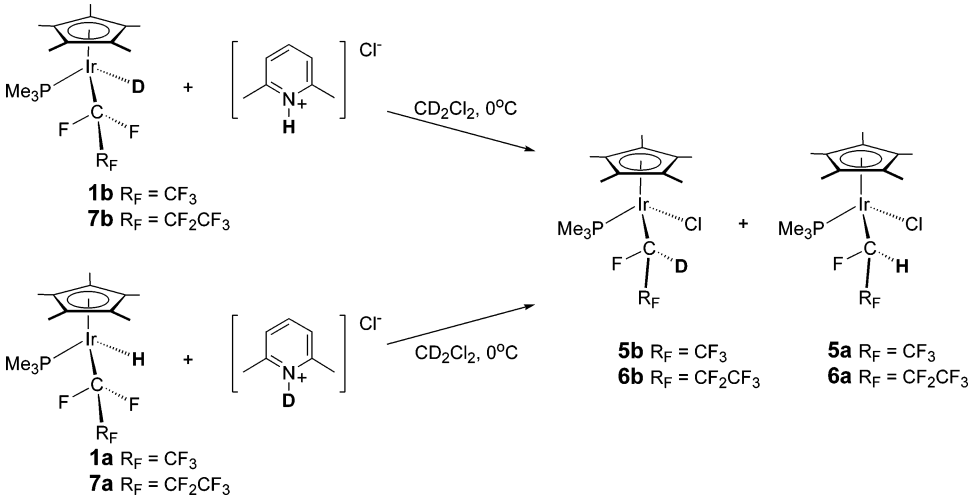

Scheme 3

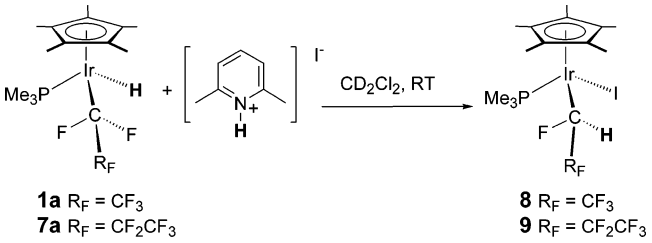

Results and Discussion

Characterization of the Diastereomeric Hydride Migration Products. Reaction of the perfluoroethyl complexes **1a** with LutDCl or **1b** with LutHCl gave compounds Cp*Ir(PMe_3)($CHFCF_3$)Cl (**5a**) and Cp*Ir(PMe_3)($CDFCF_3$)Cl (**5b**) in an *identical ratio of* ∼2:1 (Scheme 2); each compound is formed as a mixture of diastereomers, only one of which is shown, and the composition of which varies with reaction conditions (see later). Similarly a ∼2:1 mixture of complexes **6a** and **6b** was obtained from the corresponding perfluoropropyl complexes **7a** (with LutDCl) or **7b** (with LutHCl). Once formed, these diastereomeric products are configurationally stable at room temperature, and mixtures of varying ratios show no sign of equilibration.

Treatment of complexes **1a** and **7a** with >1 equiv of LutHI in CD_2Cl_2 at room temperature afforded, respectively, Cp*Ir(PMe_3)($CHFCF_3$)I (**8**) and Cp*Ir(PMe_3)($CHFCF_2CF_3$)I (**9**) as mixtures of diastereomers (ratio 1.5:1−2:1), as shown in Scheme 3. Notably, at room temperature the iodide reactions are complete before NMR spectra can be obtained and are much faster than the analogous processes with LutHCl, for which detailed kinetic measurements are possible as described below. Compound **8** has been made previously by direct oxidative addition of CF_3CFHI to Cp*Ir$(CO)_2$, followed by replacement of CO in the resultant Cp*Ir(CO)($CFHCF_3$)I by PMe_3 in refluxing toluene.[54] Notably, the diastereomer ratio obtained in this high-temperature synthesis (1:6) is inverted from the 2:1 ratio obtained by the methodology of Scheme 3. This provides some evidence that in the hydride migration reactions the principal observed diastereomer of **8**, and presumably also of **5** and **6**, is the product of kinetic control. Further kinetic evidence to confirm this is presented later. For consistency in subsequent discussion, we will henceforth refer to the major diastereomer observed in the hydride migrations (in CD_2Cl_2 solution) as the kinetic isomer and the minor one the thermodynamic isomer.

The diastereomers of complexes **5, 6, 8**, and **9** have all been fully characterized by NMR spectroscopy. For example, the ^1H NMR spectrum of complex **5a** exhibits characteristic Cp*, PMe_3, and α-CHF resonances for each diastereomer, with the α-CHF of the kinetic diastereomer resonating at δ 6.43 ppm and that of the thermodynamic diastereomer at δ 6.59 ppm; the ^{19}F spectrum shows the corresponding fluorine resonances at δ −191.5 and −192.6 ppm, respectively; the $^{31}P\{^1H\}$NMR spectrum shows the PMe_3 of the kinetic diastereomer at δ −30.2 ppm as a doublet ($^3J_{PF}$ = 21.3 Hz) from coupling with the α-fluorine, while that of the thermodynamic diastereomer appears as a broad doublet of quartets ($^3J_{PF}$ = 17, $^4J_{PF}$ = 3 Hz) at −33.2 ppm from coupling to the α-fluorine as well as the CF_3. Similarly, complex **5b** exhibits characteristic Cp* and PMe_3 resonances in the ^1H NMR spectrum; the ^2H NMR spectrum shows the α-CDF of the kinetic and thermodynamic diastereomers at δ 6.43 and 6.59 ppm, respectively, each appearing as a broad doublet ($^2J_{FD}$= 8 Hz) from coupling to the α-CDF fluorine; the ^{19}F NMR spectrum shows the α-CDF fluorine of the kinetic diastereomer at δ −192.0 ppm as a broad doublet of quartets of triplets ($^3J_{PF}$ = 22, $^3J_{FF}$ = 15, $^2J_{DF}$ = 8 Hz) from coupling with ^{31}P, CF_3, and deuterium, while the corresponding resonance for the thermodynamic diastereomer resonates at −193.6 ppm, also as a broad doublet of quartets of triplets ($^3J_{PF}$ = 17, $^3J_{FF}$ = 15, $^2J_{DF}$ = 8 Hz) from coupling with ^{31}P, CF_3, and deuterium; the $^{31}P\{^1H\}$NMR spectrum shows the resonance of the kinetic diastereomer at δ −30.2 ppm as a broad doublet ($^3J_{PF}$ = 22 Hz) from coupling to the α-CDF fluorine, whereas that of the thermodynamic diastereomer appears at −33.2 ppm as a broad doublet of quartets ($^3J_{PF}$ = 17, $^4J_{PF}$ = 3 Hz) from coupling to the α-CDF fluorine as well as the CF_3. Complexes **6a,b**, not unexpectedly, give similar spectra. For diastereomers of the iodo complex **9** the overall coupling patterns are similar to those of the chloride analogue **6a**, but in the ^1H and ^{19}F NMR spectra, most signals are shifted to higher frequency. The spectra are very similar to those of **8**, which had been previously prepared by an alternative route.[54]

The 1D NMR data for these compounds clearly define the basic connectivities but provide no definitive stereochemical

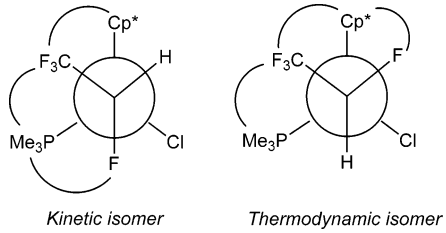

Figure 1. Newman projections down the C−Ir bond showing the major NOEs observed in the $^{19}F\{^1H\}$ HOESY experiment on **5a**. Only one enantiomer of each diastereomer is shown.

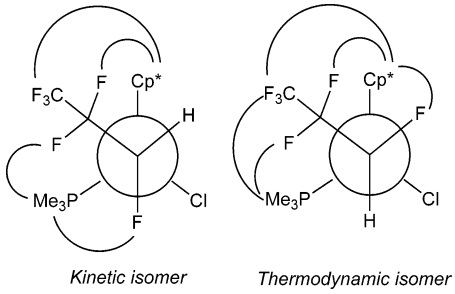

Figure 2. Newman projections down the C−Ir bond showing the major NOEs observed in the $^{19}F\{^1H\}$ HOESY experiment on **6a**. Only one enantiomer of each diastereomer is shown.

information. While we have not been able to obtain X-ray quality crystals of a single diastereomer of any of the migration products to determine the relative stereochemistries of the two stereocenters, a series of $^{19}F\{^1H\}$ HOESY studies enabled assignment of the relative configurations and preferred conformations in solution, as we have previously demonstrated for similar compounds.[68] For complexes **5a** and **6a**, the $^{19}F\{^1H\}$ HOESY experiments were performed on a mixture of diastereomers in CD_2Cl_2 solution. Newman projections of the conformations and relative stereocenter configurations derived from the observed strong NOE cross-peaks are shown in Figures 1 and 2. For **5a** NOEs were found for each isomer between the β-CF_3 and both the Cp* and P*Me*$_3$, indicating that the CF_3 is oriented between these groups. This is expected, based on numerous X-ray structures of similar compounds.[69] For the kinetic diastereomer, there is a strong NOE between the CH*F* and the P*Me*$_3$ but a much weaker NOE from CH*F* to the Cp*; the α-CF in this conformation is just within the 5 Å NOE range.[70,71] For the thermodynamic diastereomer, there is a strong NOE between the CH*F* and the Cp*, indicating they are close in space, with no correlation found from CH*F* to the P*Me*$_3$. Likewise for **6a** (Figure 2) NOEs are found from the β-CF_2 groups to both Cp* and P*Me*$_3$, indicating a close spatial relationship in each case. The CF_3 group of the thermodynamic isomer also shows a correlation to both Cp* and P*Me*$_3$; for the kinetic isomer, the CF_3 is only close to the Cp*. For the kinetic isomer, there is a strong NOE between the CH*F* and the P*Me*$_3$, demonstrating they are again close in space, while for the thermodynamic isomer there is strong correlation between the CH*F* and the Cp*, confirming that the solution conformations for **6a** are analogous to those of **5a**.

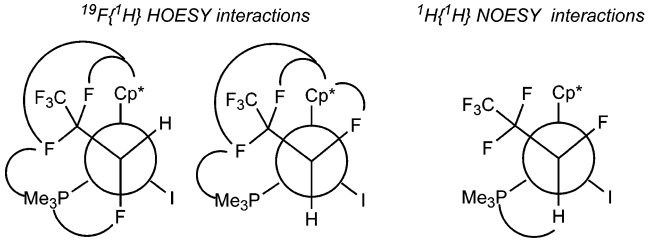

Figure 3. Newman projections down the C−Ir bond showing the major NOE interactions observed in the $^{19}F\{^1H\}$ HOESY and $^1H\{^1H\}$ NOESY experiments on **9**. Only one enantiomer of each diastereomer is shown.

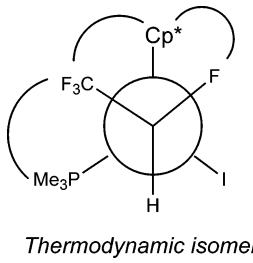

Figure 4. Newman projection down the C−Ir bond showing the major NOEs found in the $^{19}F\{^1H\}$ HOESY experiment on **8**. Only one enantiomer of this diastereomer is shown.

These NOE correlations define not only the preferred ground state *conformations* shown, but also the relative *configurations* at C and Ir for the kinetic diastereomer as (S_C, S_{Ir})(R_C, R_{Ir}) and for the thermodynamic counterpart as (R_C, S_{Ir})(S_C, R_{Ir}). In Figures 1 and 2 only the (S_C, S_{Ir}) and (R_C, S_{Ir}) isomers are depicted. It is clear that the kinetic diastereomer formed in the hydride migration reaction has the same relative stereochemistry as the single diastereomer formed in the analogous methyl migration and that this is indeed the product of kinetic control.[55]

For complex **9**, $^{19}F\{^1H\}$ HOESY and $^1H\{^1H\}$ NOESY experiments were carried out on the 2:1 mixture of diastereomers formed by reaction of **7a** with excess LutHI in CD_2Cl_2. Newman projections of the derived structures are given in Figure 3. In the $^{19}F\{^1H\}$ HOESY spectrum, NOEs were again found for each isomer between the β-CF_2 and both the Cp* and P*Me*$_3$ groups, indicating that the C_2F_5 fragment is oriented between these groups. For the thermodynamic isomer, there is a strong NOE between the CH*F* and the Cp*, with no correlation found from CH*F* to the P*Me*$_3$. For the kinetic isomer, there is a strong NOE between the CH*F* and the P*Me*$_3$, but as found for **5a**, there is also a weak NOE from CH*F* to the Cp*. In the $^1H\{^1H\}$ NOESY (Figure 3), the only significant NOE observed is between the C*HF* and the P*Me*$_3$ group of the thermodynamic isomer, consistent with the structure shown.

The $^{19}F\{^1H\}$ HOESY spectrum of the mixture of diastereomers of **8** was also obtained on the 1:6 diastereomeric mixture of **8**, formed by treatment of Cp*Ir(CO)(CHFCF$_3$)I with PMe_3 in refluxing toluene.[54] A Newman projection of the derived structure showing the main NOEs for the thermodynamic diastereomer is shown in Figure 4. In the $^1H-^{19}F$ HOESY spectrum, NOEs were seen only for the thermodynamic diastereomer but were sufficient to characterize it, and therefore by a process of elimination, the corresponding kinetic diastereomer**.** Correlations were found between the β-CF_3 and both the Cp* and P*Me*$_3$, indicating that the CF_3 fragment is oriented between these groups. A NOE is also observed between the CH*F* and

(68) Hughes, R. P.; Zhang, D.; Ward, A. J.; Zakharov, L. N.; Rheingold, A. L. *J. Am. Chem. Soc.* **2004**, *126*, 6169−6178.
(69) Hughes, R. P.; Smith, J. M.; Liable-Sands, L. M.; Concolino, T. E.; Lam, K.-C.; Incarvito, C.; Rheingold, A. L. *J. Chem. Soc., Dalton Trans.* **2000**, 873−879.
(70) Neuhaus, D.; Williamson, M. P. *The Nuclear Overhauser Effect in Structural and Conformational Analysis*; Wiley-VCH: New York, 2000.
(71) Macchioni, A. *Eur. J. Inorg. Chem.* **2003**, 195−205.

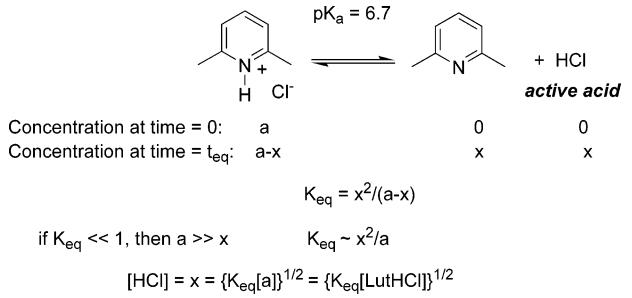

Figure 5. Interpretation of the half-order rate dependence on [LutHCl].

the Cp* ring. Thus, this isomer is analogous in structure to the thermodynamic isomers of **5a**, **6a**, and **9**, which is also apparent from their very similar NMR spectra.

With the structures of the product diastereomers firmly defined we can now move to a detailed discussion of the kinetics and mechanism of their formation and interconversion.

Kinetic Observations. We have carried out detailed kinetic studies on the reactions of **1** and **7** with LutH(D)Cl salts in three solvents: CD_2Cl_2, DMF-d_7, and CD_3NO_2. Two remarkable general observations concerning the kinetic data are worthy of initial comment. First, in all solvents the experimentally observed rate law was established to be $-d[\mathbf{Ir}]/dt = k[\mathbf{Ir}][\mathrm{LutH(D)Cl}]^{1/2}$, with an expected first-order dependence on the concentration of iridium starting complex but a surprising one-half-order dependence on the concentration of lutidinium salt. There is no literature evidence that lutidinium salts are dimeric in these solvents, so a (dimer) $\rightleftarrows$ 2(monomer) preequilibrium is not a convenient way to explain this half-order dependence. Our interpretation is summarized in Figure 5: LutHCl is a weak acid, with a pK_a(H_2O) of 6.7;[72−74] dissociation generates HCl and lutidine, the small and equal concentration of each of which has a half-order dependence on [LutHCl]. In agreement with this interpretation, addition of 2,6-lutidine results in a strong inhibition of C−F activation. *The most significant conclusion is that the active source of the exogenous proton for the C−F activation reactions is not lutidinium chloride, but rather small amounts of HCl generated by its dissociation*!

The second general observation is that plots of ln[**Ir**] versus time are *linear* for at least three reaction half-lives, even using one molar equiv of LutHCl. Clearly, the proton acts as a *catalyst* whose concentration remains effectively constant throughout most of the reaction. (As discussed later, the effect of the halide counterion must be taken into account under some circumstances.) Consequently, the raw kinetic data behave as for a pseudo first-order reaction; the slope of the linear plot gives $k_{obs}[\mathrm{LutHCl}]^{1/2}$, which in turn affords values of k_{obs}.

Initial kinetic experiments were performed for the reaction of **1a** or **7a** with LutDCl or LutHCl and **1b**[53] or **7b** with LutDCl or LutHCl in CD_2Cl_2 at 0 °C. Reactions were monitored by ^{1}H NMR, and concentrations of reactants and products were obtained by integration of appropriate resonances, using 1,3,5-trimethoxybenzene as an internal integration standard. The rate constants k_{obs} ($L^{1/2}/mol^{1/2}$ s) at 0 °C are shown in Table 1. Kinetic isotope effects are not large, and any interpretation related to the C−F activation step is clearly inappropriate due to their small magnitude and the complication that the C−F activation step is preceded by a dissociative equilibrium which will also have an unknown isotope effect associated with it.

Table 1. Rate Constants k_{obs} ($L^{1/2}/mol^{1/2}$ s) for Reaction of **1a,b** and **7a,b** with 2,6-Lutidinium(H/D) Chloride in CD_2Cl_2 at 0 °C

compound[a]	acid	$10^4\ k_{obs}$($L^{1/2}/mol^{1/2}$ s)	k_H/k_D
[Ir](H)CF_2CF_3 (**1a**)	LutHCl	7.5 ± 0.2	1.8 ± 0.2
[Ir](D)CF_2CF_3 (**1b**)	LutDCl	4.2 ± 0.2	
[Ir](D)CF_2CF_3 (**1b**)	LutHCl	5.7 ± 0.2	1.1 ± 0.2
[Ir](H)CF_2CF_3 (**1a**)	LutDCl	5.3 ± 0.2	
[Ir](H)$CF_2CF_2CF_3$ (**7a**)	LutHCl	5.8 ± 0.2	1.4 ± 0.2
[Ir](D)$CF_2CF_2CF_3$ (**7b**)	LutDCl	4.2 ± 0.2	
[Ir](D)$CF_2CF_2CF_3$ (**7b**)	LutHCl	5.6 ± 0.2	1.2 ± 0.2
[Ir](H)$CF_2CF_2CF_3$ (**7a**)	LutDCl	4.5 ± 0.2	

[a] [Ir] = Cp*Ir(PMe_3).

Scheme 4

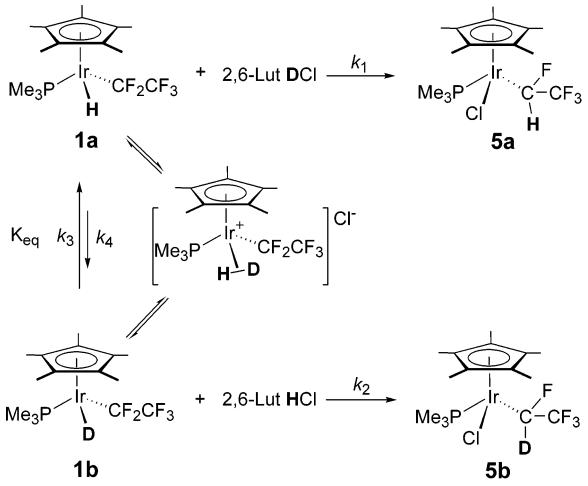

If k_3 and $k_4 \gg k_1$ and k_2; and $k_1 \sim k_2$

$$\frac{d(\mathbf{5a})/dt}{d(\mathbf{5b})/dt} = \frac{k_1[\mathbf{1a}][D^+]^{1/2}}{k_2[\mathbf{1b}][H^+]^{1/2}} = \frac{k_1[\mathbf{1a}]_{eq}[D^+]_{eq}^{1/2}}{k_2[\mathbf{1b}]_{eq}[H^+]_{eq}^{1/2}} = \frac{k_1 K_{eq}}{k_2} = K_{eq}$$

An Eyring plot of the kinetic data measured over the temperature range 0 to 15 °C affords a free energy of activation $\Delta G^{\ddagger}_{(298K)} = 84 \pm 4$ kJ mol^{-1} for the reaction of **1a** and LutHCl. An identical value of $\Delta G^{\ddagger}_{(298K)} = 85 \pm 7$ kJ mol^{-1} was obtained for the reaction of **7a** and LutHCl. These are significantly larger than the value of $\Delta G^{\ddagger}_{(298K)} = 64 \pm 2$ kJ mol^{-1} previously measured for reaction of **1a** with acetic acid, consistent with the much faster reaction (by a factor of approximately 50 at 0 °C) observed in the previously reported system.[54]

As shown in Scheme 4, the competitive proton exchange equilibrium between **1a** (**1b**) and Lut(H/D)Cl must be faster than the protonation of the α-C−F bond (k_3, $k_4 \gg k_1$, k_2), which results in complete scrambling of H and D before C−F activation, and therefore an identical mixture of **5a** and **5b** from both reactions. Similar results are observed with the corresponding perfluoropropyl analogues **7a,b**. Clearly, when k_1 is similar to k_2, the degree of isotopic scrambling in the final products (**5a** and **5b)** is determined by the equilibrium isotope effect in the proton exchange equilibrium between **1a** (**1b**) and Lut(H/D)Cl. In other words, the isotopomer ratio [**5a**]/[**5b**] reflects the equilibrium constant (K_{eq}) for the H/D exchange process. This is different from the previously reported system

(72) Gero, A.; Markham, J. J. *J. Org. Chem.* **1951**, *16*, 1835−1838.
(73) Brown, H. C.; Mihm, X. R. *J. Am. Chem. Soc.* **1955**, *77*, 1723−1726.
(74) Brown, H. C.; Kanner, B. *J. Am. Chem. Soc.* **1966**, *88*, 986−992.

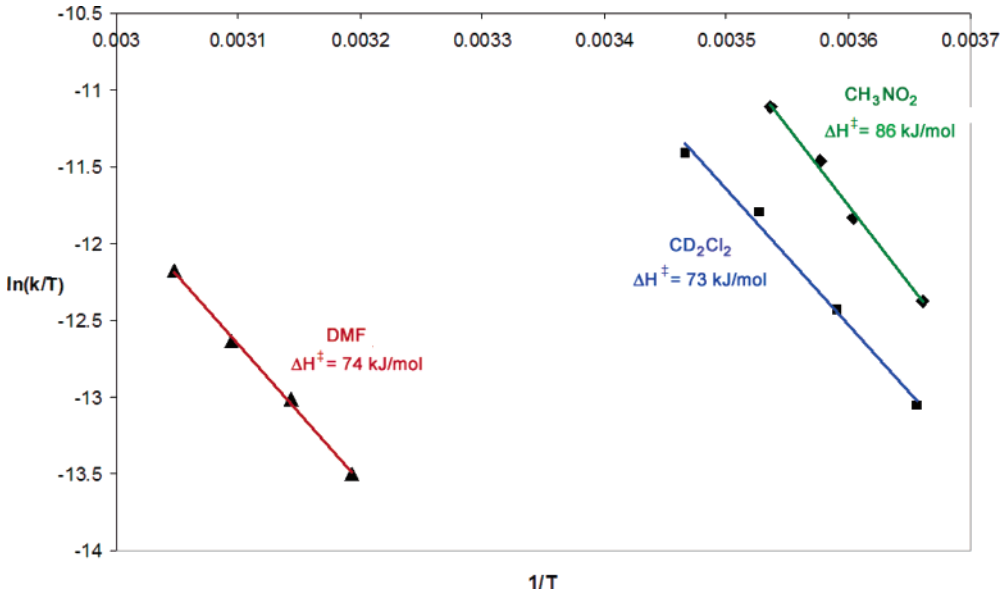

Figure 6. Eyring plots for the reaction of **7a** with LutHCl in different solvents.

Table 2. Solvent Effects on the Activation Parameters for the Reaction of Cp*Ir(PMe$_3$)(C$_3$F$_7$)H (7a) + LutHCl

solvent	donor no. (kJ mol^{-1})[a]	dielectric constant ϵ_r[a]	$\Delta H^{\ddagger}$ (kJ mol^{-1})	$\Delta S^{\ddagger}$ (J mol^{-1} K^{-1})	$\Delta G^{\ddagger}_{(298K)}$ (kJ mol^{-1})
CD_2Cl_2	0	8.9	73(5)	−38(18)	85(7)
CD_3NO_2	11.3	35.9	86(4)	14(15)	82(6)
DMF-d_7	111.3	36.7	74(2)	−73(7)	96(3)

[a] Ref 77.

using acetic acid as the protonating agent, in which the corresponding k_1 and k_2 values must be larger than k_3 or k_4 and scrambling competes very inefficiently with C−F bond activation.[54] The exchange is shown as occurring via a putative cationic η^2-HD intermediate, which is not directly observed in this system. However similar cationic species, obtained by protonation of iridium hydrides, have been reported elsewhere.[75,76]

Solvent effects on the overall reaction rates were significant; compared to reactions in CD_2Cl_2 those in DMF-d_7 were considerably slower and those in CD_3NO_2 considerably faster. As already mentioned, the experimental rate law is identical in all three solvent systems. Eyring plots are shown in Figure 6 for the reaction of **7a** with LutHCl in the three solvents used.

Values of $\Delta H^{\ddagger}$ and $\Delta S^{\ddagger}$ obtained from these plots were used to calculate $\Delta G^{\ddagger}_{(298K)}$ for each reaction; the results, along with values of the donor number and dielectric constants for each solvent,[77] are compared in Table 2. Clearly the overall activation free energies are strongly influenced by the sign of the $\Delta S^{\ddagger}$ term. While the values of $\Delta G^{\ddagger}$ in CD_2Cl_2 and in CD_3NO_2 are statistically indistinguishable, reaction rates are observed to be significantly faster in the latter solvent, and while the uncertainty in the calculated $\Delta G^{\ddagger}$ values do not reflect this in a statistically different way, it is clear that the relative values of $\Delta G^{\ddagger}$ are $CD_3NO_2 < CD_2Cl_2$. It is also clear that the faster reaction in CD_3NO_2 compared to CD_2Cl_2 is a result of the sign of the $\Delta S^{\ddagger}$ component rather than the $\Delta H^{\ddagger}$ values. Likewise, the significantly greater value for $\Delta G^{\ddagger}$ when DMF-d_7 is used as the solvent is also a result of the large negative value of $\Delta S^{\ddagger}$ in this solvent. Comparison of rates using CD_3NO_2 and DMF-d_7 makes it clear that solvent donor properties and dielectric constants are both important in affecting the reaction rate. It seems likely that strong donor solvent stabilization of the protic acid component of the starting materials will be a significant cause of slower reaction rates in DMF. As we will see shortly, the intermediate formed by C−F activation must be ionic and therefore the transition state leading to this intermediate must be a polar one. In DMF the large negative $\Delta S^{\ddagger}$ and consequently slower rate could result from the solvation requirements for this transition state, while in nitromethane the high solvent dielectric helps to stabilize this relative to the ground state.

Plots of concentration versus time for the reaction of **7a** with varying amounts of LutHCl in CD_2Cl_2, two examples of which are shown in Figure 7, provide considerable insight into the nature of the intermediates from which the kinetic ($R_{Ir}R_C$, $S_{Ir}S_C$) and thermodynamic ($R_{Ir}S_C$, $S_{Ir}R_C$) diastereomeric products are formed. When an excess of LutHCl (4.6 equiv) is used, the plot shows the expected features, with a pseudo first-order decay of starting material **7a** and formation of the kinetic and thermodynamic diastereomers of product **6a**. When a smaller excess of LutHCl (2.0 equiv) is used, the ratio of diastereomers of **6a** varies over the reaction course, as shown in Figure 8, starting at ∼4:1 (by extrapolation) and giving a final ratio of ∼2.5:1. When a larger excess of LutHCl (10 equiv) is used, the ratio of diastereomers remains constant at ∼4:1 over the entire reaction course. Recall that we have shown that, once isolated from the reaction mixture, the product diastereomers do not interconvert or equilibrate at room temperature. However, as shown in Figure 7, when using less than one equiv of LutHCl it is clear that in the very late stages of the reaction *the kinetic product diastereomer is actually consumed to produce its thermodynamic counterpart; the sudden divergence in the concentrations appears to coincide with the time at which the concentration of available chloride drops to approximately zero.*

(75) Tellers, D. M.; Bergman, R. G. *Organometallics* **2001**, *20*, 4819−4832.
(76) Oldham, W. J., Jr.; Hinkle, A. S.; Heinekey, D. M. *J. Am. Chem. Soc.* **1997**, *119*, 11028−11036.
(77) Reichardt, C. *Solvents and Solvent Effects in Organic Chemistry*; Wiley-VCH: Weinheim, Germany, 2003.

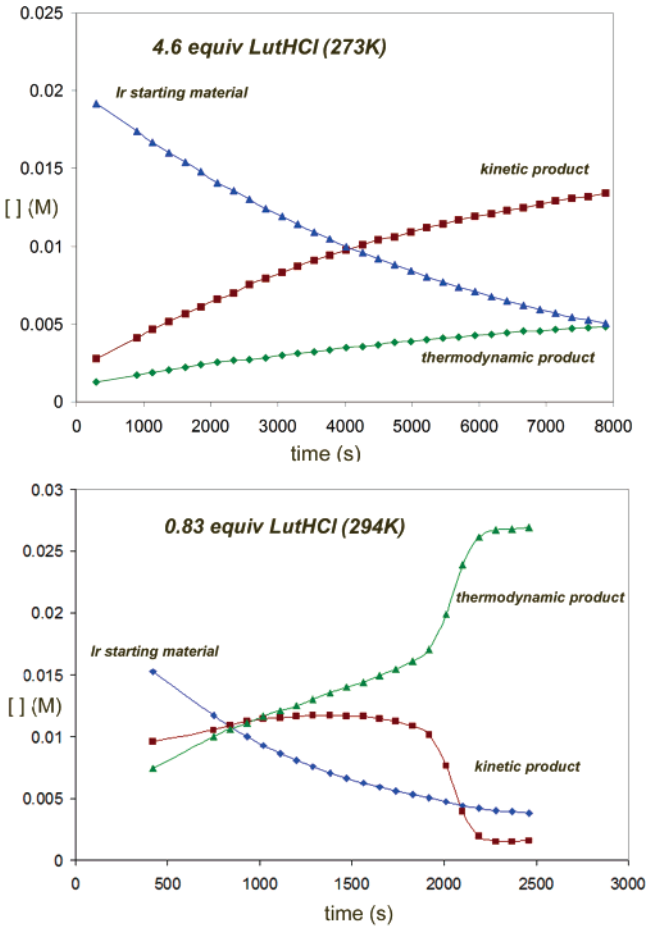

Figure 7. Plots of concentration vs time for starting materials and diastereomeric products in the reactions of **7a** with two different equiv of LutHCl in CD_2Cl_2.

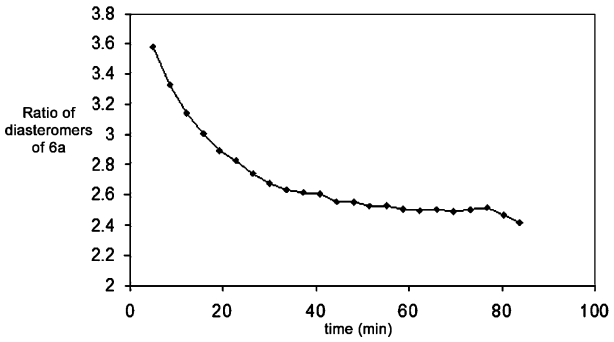

Figure 8. Variation of the ratio of diastereomers of product **6a** in the reaction of **7a** with 2.0 equiv of LutHCl in CD_2Cl_2 at 15 °C.

The Reaction Mechanism. A reaction mechanism consistent with the observed kinetic results is shown in Scheme 5 using the *S*-enantiomer of racemic starting complex **1a** or **7a**; obviously a mirror image scheme must exist for the corresponding *R*-enantiomer. In a previously published study of C−F bond activation reactions of **7a** coupled with vinyl migration, we have provided evidence that the *S*-enantiomer of the starting material affords the *S*-configuration at carbon in the product and that C−F bond activation is completely diastereoselective.[67] We have no reason to suppose that hydride migration should proceed by a fundamentally different pathway, and so Scheme 5 depicts an analogous, selective loss of F_a and migration of H to give cation $\mathbf{10}_{SS}$ as the kinetically formed intermediate. Irreversible

Scheme 5

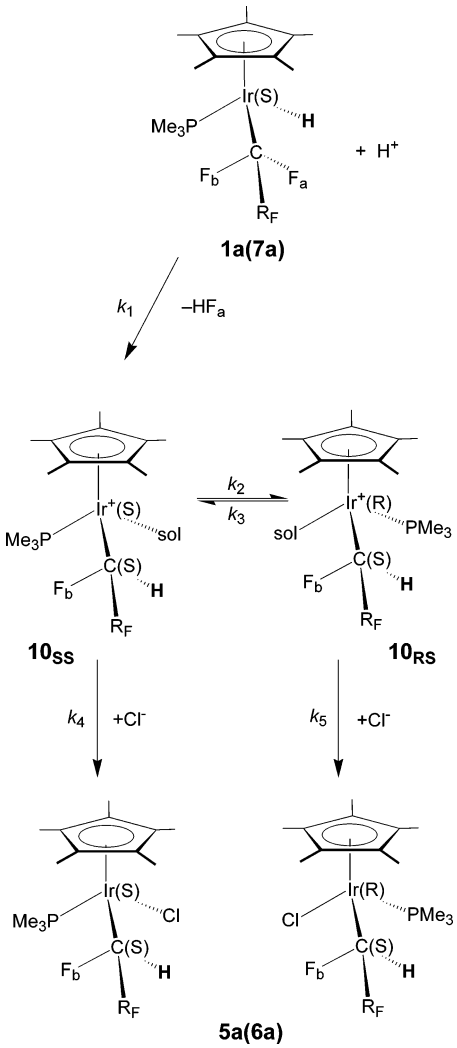

trapping of $\mathbf{10}_{SS}$ by chloride would afford the observed kinetic diastereomer of **5a (6a)**. However, if inversion at iridium occurs before chloride trapping, $\mathbf{10}_{SS}$ forms $\mathbf{10}_{RS}$, which can then be trapped by chloride to give the thermodynamic product diastereomer. In previous work we have shown that inversion at the metal in such 16-electron cations can be fast on the NMR time scale.[78] In Scheme 5 the cationic intermediates **10** are shown as being solvated, even in CD_2Cl_2, as analogous weakly bound methylene chloride and other chlorocarbon complexes have been experimentally observed in alkyl analogues of **10**.[75,79−82]

To ensure that changes in the diastereomeric ratio are not due to any configurational lability of the α-carbon under the reaction conditions, isolated **6a** was treated with LutDCl to test whether deuterium incorporation into the α-carbon occurs through a proton exchange pathway. No deuterium was observed in **6a** after 24 h. This is consistent with the idea that configurational inversion at iridium is responsible for the change in diastereomer ratio during the reaction.

(78) Hughes, R. P.; Lindner, D. C.; Rheingold, A. L.; Liable-Sands, L. M. *J. Am. Chem. Soc.* **1997**, *119*, 11544−11545.
(79) Arndtsen, B. A.; Bergman, R. G. *Science* **1995**, *270*, 1970−1973.
(80) Tellers, D. M.; Bergman, R. G. *Can. J. Chem.* **2001**, *79*, 525−528.
(81) Tellers, D. M.; Bergman, R. G. *J. Am. Chem. Soc.* **2001**, *123*, 11508−11509.
(82) Tellers, D. M.; Yung, C. M.; Arndtsen, B. A.; Adamson, D. R.; Bergman, R. G. *J. Am. Chem. Soc.* **2002**, *124*, 1400−1410.

Therefore, formation of two diastereomers throughout the reaction appears to result from competition between intramolecular inversion at iridium in initially formed cationic intermediate $\mathbf{10}_{SS}$ and bimolecular trapping of that intermediate by chloride. This is consistent with the observation that using larger excesses of LutHCl results in an approximately constant ratio of product diastereomers throughout the reaction but that reduction of the concentration of LutHCl, and hence the concentration of chloride available for trapping, results in reduced rates of bimolecular trapping relative to inversion at iridium and consequently a decrease in the kinetic/thermodynamic diastereomer ratio over time (Figure 8). The rate of inversion ($k_2[\mathbf{10}_{SS}]$) must be similar to that for trapping of the cationic intermediate $\mathbf{10}_{SS}$ by chloride ($k_4[\mathbf{10}_{SS}][Cl^-]$) (see Scheme 5). If the rate of inversion were much faster than that for trapping, the diastereomer ratio would reflect the equilibrium constant ($K_{eq} = k_3/k_4$) for inversion and should not change with time, assuming that the rates of trapping of $\mathbf{10}_{SS}$ and $\mathbf{10}_{RR}$ were essentially the same. If the rate constants of inversion (k_2, k_3) and trapping (k_4, k_5) are similar, then as $[Cl^-]$ decreases, one would expect to see a change in product diastereomer ratio. This change will be greater if intermediate $\mathbf{10}_{RS}$ is favored thermodynamically over $\mathbf{10}_{SS}$; i.e., if $k_2 > k_3$.

If potentially equilibrating cationic intermediates **10** are indeed formed, significant solvent effects are expected, and they are observed. Reactions are at least twice as fast in the higher dielectric constant solvent CD_3NO_2 (vide supra) consistent with a polar intermediate, and significantly, the diastereomer ratio is inverted compared to that observed in CD_2Cl_2 under similar conditions. The use of 2 equiv of LutHCl in CD_2Cl_2 gives an initial kinetic/thermodynamic diastereomer ratio of **6a** of ~4:1 decreasing to ~2:1; in CD_3NO_2 the ratio is initially 2:3, changing over the reaction course to 1:2. This is consistent with the polar intermediate **10** (see Scheme 5) formed after C−F activation/migration being stabilized in nitromethane, allowing intramolecular epimerization at iridium to occur more competitively with chloride trapping. Support for this mechanistic premise was provided when a 3:2 mixture of kinetic/thermodynamic diastereomers of **6a**, generated in CD_2Cl_2 was observed to be unchanged after 1 day. On dissolution of this same mixture in CD_3NO_2, a rapid change in diastereomer ratio to 1:2 was found; this changed steadily over 3 days until it reached an apparent equilibrium value of ~1:15. This is clearly indicative of irreversible coordination of chloride and consequent configurational stability at iridium in CD_2Cl_2, but reversible dissociation of chloride in nitromethane, allowing thermodynamic control of the diastereomer ratio to prevail via epimerization at iridium.

In DMF-d_7, reactions of **7a** with LutHCl were, as mentioned earlier, much slower than in CD_2Cl_2, but diastereomer ratios of 2:1 were typically found not to change over the course of the reaction. Unlike reactions in methylene chloride or nitromethane, epimerization at iridium does not appear to occur over time, perhaps because any intermediate cation is configurationally stabilized by stronger coordination of DMF than either CD_2Cl_2 or CD_3NO_2.

Finally, any mechanism must account for the observation that, while the individual product diastereomers are configurationally stable in CD_2Cl_2, reactions using less than one equiv of LutHCl result in sudden, rapid conversion of the kinetic product to the thermodynamic product once the concentration of chloride drops to approximately zero (Figure 7). This can occur if untrapped cation $\mathbf{10}_{SS}$ (or $\mathbf{10}_{RS}$) can catalyze this transformation, presumably via a halide-bridged intermediate **11**, as shown in Scheme 6. By halide exchange via the bridged species **11**, a cation such as $\mathbf{10}_{RS}$ can convert the configurationally stable kinetic diastereomer shown into a configurationally labile cation $\mathbf{10}_{SS}$; if this reaction is reasonably fast it must result in conversion of kinetic product diastereomer to the thermodynamic diastereomer. To test this premise, a 2:1 diastereomer mixture of **6a** was treated with 0.1 equiv of $Cp^*Ir(PMe_3)(C_3F_7)(O_3SCF_3)$[55] in CD_2Cl_2 at 21 °C in an NMR tube. The triflate ligand is weakly bound, and this complex should be an appropriate substitute for the cationic intermediate **10** in the hydride migration reactions. A ^1H NMR spectrum obtained within 5 min of mixing showed a dramatic change in the diastereomer ratio of **6a** from 2:1 to <1:10, consistent with our prediction. The above results support our proposal that halide exchange with a cationic intermediate is responsible for the epimerization observed when $[Ir] > [Cl^-]$.

Attempts were made to isolate the cationic intermediate **10** by treatment of **7a** with 1 equiv of $LutH[B\{3,5\text{-}C_6H_3(CF_3)_2\}_4]$,[83] containing a very weakly coordinating anion, in CD_2Cl_2 at room temperature. The reaction was complete within minutes, apparently giving $[Cp^*Ir(PMe_3)(CHFC_2F_5)]^+[B\{3,5\text{-}C_6H_3(CF_3)_2\}_4]^-$. Like other analogues[75,79−82] (vide supra), it is probable that this species contains a coordinated molecule of CD_2Cl_2. The ^1H

Scheme 6

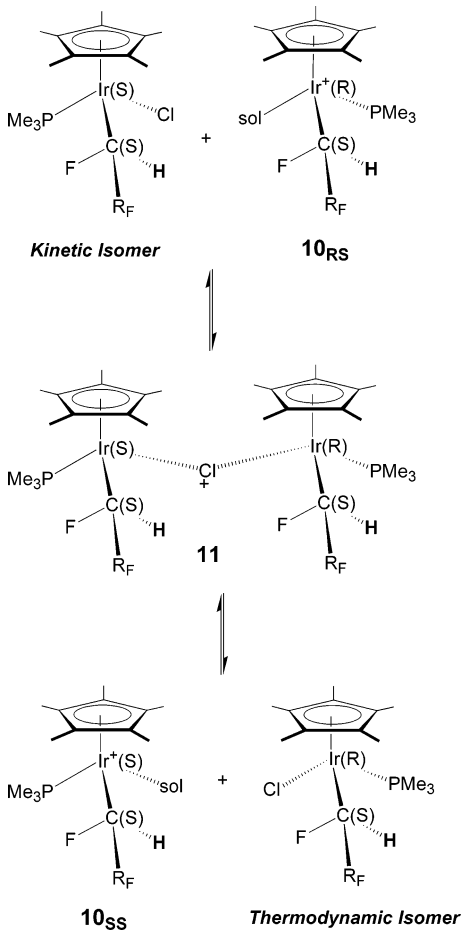

(83) Yandulov, D. V.; Schrock, R. R. *J. Am. Chem. Soc.* **2002**, *124*, 6252−6253.

Scheme 7. Mechanism and Rate Constants (CD_2Cl_2; 294 K) from Simulation Using the IBM CKS Program[a,b]

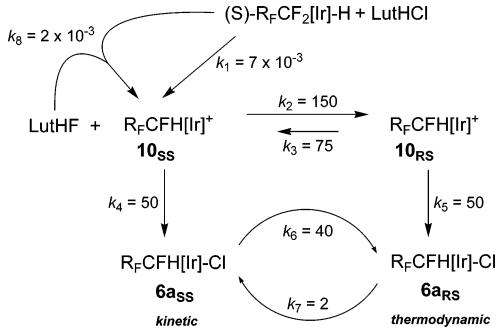

[a] Ref 84. [b] k_6 and k_7 are rate constants for interconversion of diastereomers of product by untrapped cations **10**.

NMR spectrum showed a single set of resonances for an iridium complex: doublets at δ 1.72 and 1.58 for the Cp* and P*Me*$_3$, respectively, and a doublet of doublets at δ 6.81 for the α-C*H*F. In the ^{19}F NMR spectrum, a sharp singlet was found at −83.3 ppm for the CF_3 group of the iridium complex along with broad resonances at −112.6 and −116.5 ppm due to the β-CF_2 group and a broad multiplet at −193.0 ppm due to the α-CH*F*. The ^{31}P NMR spectrum showed a single peak, at −24.37 ppm, consistent with a cationic iridium complex. On leaving the product from reaction of **7a** and LutH$^+$[B{3,5-$C_6H_3(CF_3)_2$}$_4$]$^-$ in CD_2Cl_2 solution for 30 min, some chloride abstraction from the solvent was observed to give complex **6a**. Addition of 1 equiv of NaI in CD_3OD at this point produced **9** as a 1:15 mixture of diastereomers, i.e., the thermodynamic isomer favored.

In summary, we conclude that iridium cations **10** are crucial intermediates during these C−F activation/hydride migration reactions and play two key roles in the epimerization at iridium and consequent loss of reaction diastereoselectivity; intramolecular inversion of the cation competes with chloride trapping, and untrapped cation also catalyzes the interconversion of product diastereomers. This loss can be minimized by using high concentrations of LutHCl but not eliminated altogether.

The proposed mechanism was subjected to testing using the IBM chemical kinetics simulator.[84] The mechanism shown in Scheme 7 with the rate constants shown give satisfactory simulations of the concentration versus time data for all reagents and products in CD_2Cl_2 at 294 K, such as those shown in Figure 8; in particular it is successful in the challenging simulation of the data using less than 1 equiv of LutHCl, in which dramatic concentration changes of product diastereomers occur late in the reaction. The mechanism requires selective C−F bond activation with hydride migration to give cation $\mathbf{10}_{SS}$ to be rate limiting, with the subsequent inversion at iridium and trapping by halide being significantly faster processes. The simulations are based on reasonable estimates for some key rate constants; the overall rate constant k_{obs} from reactions at 273 K was extrapolated to give a reasonable estimate for the room-temperature value of k_1, and the rate of inversion at iridium in the known cationic complex [Cp*Ir(PMe_3)(CF_2CF_3)-(H_2O)]$^+$(BF_4)$^-$ is fast on the NMR time scale with an estimated rate constant of $\sim 10^3$ s^{-1}.[85] The use of these as initial estimates for the rate constants (k_1, k_2, k_3) allowed appropriate values for other rate constants to be derived to give the best fit. Interestingly, to get a satisfactory fit, a value of k_8 ($< k_1$) for protonation of starting material by putative product LutHF was required. This is relatively insignificant when excess LutHCl is used. Rate constants for inversion at iridium (k_2, k_3) are somewhat larger than those for trapping by chloride (k_4, k_5). The ratio of k_6/k_7 also reflects the approximate equilibrium constant ($\sim$15) for the thermodynamic/kinetic diastereomer products, albeit measured in CD_3NO_2 instead of CD_2Cl_2.

Conclusions

Major features of the mechanism of exogenous proton-promoted C−F bond activation coupled with hydride migration at iridium have been clarified. The half-order dependence on LutHCl concentration strongly suggests that LutHCl is not the active source of protons but rather dissociates to provide small concentrations of HCl as the active reagent. Kinetic and thermodynamic product stereochemistries have been defined clearly, and in particular the reasons for less than complete diastereoselectivity have been elucidated. These results beg the question of why diastereoselectivity is so clean in other migrating group systems, and experiments designed to probe these other reactions are underway. These results are also not able to distinguish whether C−F bond activation and H-migration occur in a synchronous or sequential fashion. Further experiments to examine this question are underway.

Experimental Section

General Considerations. All reactions were performed in oven-dried glassware, using standard Schlenk techniques, under an atmosphere of nitrogen which has been deoxygenated over BASF catalyst and dried over Aquasorb, or in a Braun drybox. Methylene chloride, hexane, diethyl ether, tetrahydrofuran, and toluene were dried over an alumina column under nitrogen.[86] NMR spectra were recorded on a Varian Unity Plus 300 or 500 MHz FT spectrometer. ^{1}H NMR spectra were referenced to the protio impurity in the solvent; C_6D_6 (7.16 ppm), $CDCl_3$ (7.27 ppm), CD_2Cl_2 (5.32 ppm). ^{19}F NMR spectra were referenced to external $CFCl_3$ (0.00 ppm). ^{31}P{^{1}H} NMR spectra were referenced to external 85% H_3PO_4 (0.00 ppm). The complexes Cp*Ir(PMe_3)(CF_2CF_3)H (**1a**), Cp*Ir(PMe_3)(CF_2CF_3)D (**1b**), Cp*Ir(PMe_3)($CF_2CF_2CF_3$)H (**7a**), and Cp*Ir(PMe_3)($CF_2CF_2CF_3$)D (**7b**)[53] were prepared by literature procedures. Cp*Ir(PMe_3)($CHFCF_3$)I (**8**) had been previously synthesized, by an alternative route.[54] LutHCl, LutDCl,[87] and Lut-[B{3,5-$C_6H_3(CF_3)_2$}$_4$][83] were prepared according to literature procedures.

2,6-Lutidinium Iodide. To a solution of 2,6-lutidine (1.2 mL, 10.2 mmol) in THF (25 mL) was added methanol (0.62 mL, 15.25 mmol) followed by trimethylsilyliodide (3.05 g, 15.25 mmol), each via syringe. Immediate evolution of HI and precipitation of a white powder was observed. The mixture was stirred for 30 min and then filtered via cannula. The solid was washed 4 times with THF (10 mL) and then dried in vacuo. The solid was recrystallized from CH_2Cl_2/hexane to yield a pale yellow microcrystalline solid, yield 1.45 g (60%). ^{1}H NMR ($CDCl_3$): δ 14.25 (br s, 1H, Lut*H*$^+$), 8.29 (t, J = 7.8 Hz, 1H, *p*-Py*H*), 7.59 (d, J = 7.8 Hz, 2H, *m*-Py*H*), 3.05 (s, 6H, Py*Me*).

(84) Hinsberg, W. D.; Houle, F. A. IBM Almaden Research Center Chemical Kinetics Simulator. https://www.almaden.ibm.com/st/computational_science/ck/msim/, September 2005.

(85) Hughes, R. P.; Lindner, D. C.; Smith, J. M.; Zhang, D.; Incarvito, C. D.; Lam, K.-C.; Liable-Sands, L. M.; Sommer, R. D.; Rheingold, A. L. *J. Chem. Soc., Dalton Trans.* **2001**, 2270−2278.

(86) Pangborn, A. B.; Giardello, M. A.; Grubbs, R. H.; Rosen, R. K.; Timmers, F. J. *Organometallics* **1996**, *15*, 1518−1520.

(87) Gronberg, K. L. C.; Henderson, R. A.; Oglieve, K. E. *J. Chem. Soc., Dalton Trans.* **1998**, 3093−3104.

Cp*Ir(PMe$_3$)(CHFCF$_3$)Cl (5a). A J-Young NMR tube was charged with Cp*Ir(PMe$_3$)(CF$_2$CF$_3$)H (9.1 mg, 0.0174 mmol) and LutHCl (2.5 mg, 0.0174 mmol). CD_2Cl_2 (0.5 mL) was vacuum transferred into the NMR tube. After about 1 h at room temperature, the NMR spectra showed the complete conversion of Cp*Ir(PMe$_3$)(CF$_2$CF$_3$)H into Cp*Ir(PMe$_3$)(CHFCF$_3$)Cl as a 2.7:1 mixture of two diastereomers. The ratio of the two diastereomers changed over the reaction period, from 4.3:1 to 2.7:1. The solvent was pumped down, and the yellow residue was extracted into hexane. Evaporation of hexane afforded a yellow solid (9.3 mg, 99%). Anal. Calcd for $C_{15}H_{25}ClF_4IrP$ (540.00): C, 33.36; H, 4.67. Found: C, 33.49; H, 4.64.

The kinetic diastereomer (S_C, S_{Ir})(R_C, R_{Ir}): ^{1}H NMR (CD_2Cl_2) δ 6.43 (dqd, $^2J_{FH}$ = 47, $^3J_{FH}$ = 12, $^3J_{PH}$ = 6, 1H, CHF), 1.68 (d, $^4J_{PH}$ = 2, 15H, Cp*), 1.57 (d, $^2J_{PH}$ = 11, 9H, PMe$_3$); ^{19}F NMR (CD_2Cl_2) δ −71.0 (dd, $^3J_{FF}$ = 13, $^3J_{HF}$ = 12, 3F, CF$_3$), −191.5 (ddq, $^2J_{HF}$ = 47, $^3J_{PF}$ = 21, $^3J_{FF}$ = 15, 1F, CHF); ^{31}P{^{1}H}NMR (CD_2Cl_2) δ −30.2 (d, $^3J_{PF}$ = 21, PMe$_3$).

The thermodynamic diastereomer (R_C, S_{Ir}) (S_C, R_{Ir}): ^{1}H NMR (CD_2Cl_2) δ 6.59 (dqd, $^2J_{FH}$ = 47, $^3J_{FH}$ = 11, $^3J_{PH}$ = 3, 1H, CHF), 1.72 (d, $^4J_{PH}$ = 2, 15H, Cp*), 1.47 (d, $^2J_{PH}$ = 11, 9H, PMe$_3$); ^{19}F NMR (CD_2Cl_2) δ −71.1 (ddd, $^3J_{FF}$ = 15, $^3J_{HF}$ = 11, $^4J_{PF}$ = 4, 3F, CF$_3$), −192.9 (ddq, $^2J_{HF}$ = 47, $^3J_{PF}$ = 17, $^3J_{FF}$ = 15, 1F, CHF); ^{31}P{^{1}H}NMR (CD_2Cl_2) δ −33.2 (dq, $^3J_{PF}$ = 17, $^4J_{PF}$ = 4, PMe$_3$).

Cp*Ir(PMe$_3$)(CDFCF$_3$)Cl (5b). A J-Young NMR tube was charged with Cp*Ir(PMe$_3$)(CF$_2$CF$_3$)D (9.1 mg, 0.0174 mmol) and LutDCl (2.5 mg, 0.0174 mmol). CD_2Cl_2 (0.5 mL) was vacuum transferred into the NMR tube. After about 1 h at room temperature, the NMR spectra showed the complete conversion of Cp*Ir(PMe$_3$)(CF$_2$CF$_3$)D into Cp*Ir(PMe$_3$)(CDFCF$_3$)Cl as a 2.5:1 mixture of a two diastereomers. The solvent was pumped down, and the yellow residue was extracted into hexane. Evaporation of hexane afforded a yellow solid (9.3 mg, 99%). Anal. Calcd for $C_{15}H_{24}DClF_4IrP$ (541.03): C, 33.30; H, 4.66. Found: C, 33.46; H, 4.69.

The kinetic diastereomer: ^{2}H NMR (CH_2Cl_2) δ 6.43 (br d, $^2J_{FD}$ = 8, CDF); ^{1}H NMR (CD_2Cl_2) δ 1.68 (d, $^4J_{PH}$ = 2, 15H, Cp*), 1.57 (d, $^2J_{PH}$ = 11, 9H, PMe$_3$); ^{19}F NMR (CD_2Cl_2) δ −71.0 (br d, $^3J_{FF}$ = 15, 3F, CF$_3$), −192.0 (br dqt, $^3J_{PF}$ = 22, $^3J_{FF}$ = 15, $^2J_{DF}$ = 8, 1F, CDF); ^{31}P{^{1}H}NMR (CD_2Cl_2) δ −30.2 (br d, $^3J_{PF}$ = 22, PMe$_3$).

The thermodynamic diastereomer: ^{2}H NMR (CH_2Cl_2) δ 6.59 (br d, $^2J_{FD}$ = 8, 1D, CDF); ^{1}H NMR (CD_2Cl_2) δ 1.72 (d, $^4J_{PH}$ = 2, 15H, Cp*), 1.47 (d, $^2J_{PH}$ = 11, 9H, PMe$_3$); ^{19}F NMR (CD_2Cl_2) δ −71.2 (br dd, $^3J_{FF}$ = 15, $^4J_{PF}$ = 3, 3F, CF$_3$), −193.6 (br dqt, $^3J_{PF}$ = 17, $^3J_{FF}$ = 15, $^2J_{DF}$ = 8, 1F, CDF); ^{31}P{^{1}H}NMR (CD_2Cl_2) δ −33.2 (br dq, $^3J_{PF}$ = 17, $^4J_{PF}$ = 3, PMe$_3$).

Cp*Ir(PMe$_3$)(CHFCF$_2$CF$_3$)Cl (6a). A J-Young NMR tube was charged with Cp*Ir(PMe$_3$)(CF$_2$CF$_2$CF$_3$)H (10 mg, 0.0174 mmol) and 2,6-lutidinium(H) chloride (5 mg, 0.0348 mmol). CD_2Cl_2 (0.4 mL) was vacuum transferred into the NMR tube. After about 1 h at room temperature, the NMR spectra showed the complete conversion of Cp*Ir(PMe$_3$)(CF$_2$CF$_2$CF$_3$)H into Cp*Ir(PMe$_3$)(CHFCF$_2$CF$_3$)Cl as a 2.4:1 mixture of two diastereomers. The solvent was pumped down, and the yellow residue was extracted into hexane. Evaporation of hexane afforded a yellow solid (10 mg, 99%). The diastereomeric ratio changed over the reaction course, from 3.7:1 to 2.4:1 Anal. Calcd for $C_{16}H_{25}ClF_6IrP$ (590.01): C, 32.57; H, 4.27. Found: C, 32.68; H, 4.09.

The kinetic diastereomer: ^{1}H NMR (CD_2Cl_2) δ 6.57 (ddd, $^2J_{FH}$ = 47, $^3J_{FH}$ = 38, $^3J_{PH}$ = 5, 1H, CHF), 1.66 (d, $^4J_{PH}$ = 2, 15H, C$_5$Me$_5$), 1.56 (d, $^2J_{PH}$ = 11, 9H, PMe$_3$); ^{19}F NMR (CD_2Cl_2) δ −83.13 (d, $^4J_{FF}$ = 12, 3F, CF$_3$), −115.26 (dd, $^2J_{FF}$ = 273, $^3J_{FF}$ = 20, 1F, β-CF), −118.09 (ddd, $^2J_{FF}$ = 273, $^3J_{FH}$ = 38, $^3J_{FF}$ = 18, 1F, β-CF), −195.95 (br s, 1F, CHF); ^{31}P{^{1}H}NMR (CD_2Cl_2) δ −30.56 (d, $^3J_{PF}$ = 20, PMe$_3$).

The thermodynamic diastereomer: ^{1}H NMR (CD_2Cl_2) δ 6.75 (ddd, $^2J_{FH}$ = 48, $^3J_{FH}$ = 40, $^3J_{PH}$ = 3, 1H, CHF), 1.72 (d, $^4J_{PH}$ = 2, 15H, C$_5$Me$_5$), 1.45 (d, $^2J_{PH}$ = 10, 9H, PMe$_3$); ^{19}F NMR (CD_2Cl_2) δ −82.94 (d, $^4J_{FF}$ = 13, 3F, CF$_3$), −112.45 (ddd, $^2J_{FF}$ = 274, $^4J_{FP}$ = 21, $^3J_{FF}$ = 21, 1F, β-CF), −116.70 (ddd, $^2J_{FF}$ = 274, $^3J_{FH}$ = 40, $^3J_{FF}$ = 17, 1F, β-CF), −194.43 (br s, 1F, CHF); ^{31}P{^{1}H}NMR (CD_2Cl_2) δ −34.0 (dd, $^3J_{PF}$ = 21, $^4J_{PF}$ = 21, PMe$_3$).

Cp*Ir(PMe$_3$)(CHFCF$_2$CF$_3$)I (9). A J-Young NMR tube was charged with Cp*Ir(PMe$_3$)(CF$_2$CF$_2$CF$_3$)H (10 mg, 0.0174 mmol) and LutHI (8 mg, 0.0348 mmol). CD_2Cl_2 (0.5 mL) was transferred into the NMR tube by syringe. After 10 min, the NMR spectra showed the complete conversion of Cp*Ir(PMe$_3$)(CF$_2$CF$_2$CF$_3$)H into Cp*Ir(PMe$_3$)(CHFCF$_2$CF$_3$)I as a 2:1 mixture of two diastereomers. The solvent was pumped down, and the yellow residue was extracted into hexane. Evaporation of hexane afforded a yellow solid (12 mg, 99%). Anal. Calcd for $C_{16}H_{25}ClF_6IIrP$ (681.46): C, 28.20; H, 3.70. Found: C, 28.08; H, 3.62.

The kinetic diastereomer: ^{1}H NMR (CD_2Cl_2) δ 6.94 (ddd, $^2J_{FH}$ = 47.5 Hz, $^3J_{FH}$ = 33.8 Hz, $^3J_{PH}$ = 2.5, 1H, CHF), 1.90 (d, $^4J_{PH}$ = 2 Hz, 15H, C$_5$Me$_5$), 1.78 (d, $^2J_{PH}$ = 11 Hz, 9H, PMe$_3$); ^{19}F NMR (CD_2Cl_2) δ −83.43 (d, $^4J_{FF}$ = 17 Hz, 3F, CF$_3$), −109.91 (dd, $^2J_{FF}$ = 273 Hz, $^3J_{FF}$ = 17 Hz, 1F, β-CF), −118.09 (ddd, $^2J_{FF}$ = 273 Hz, $^3J_{FF}$ = 33.8 Hz, $^3J_{FF}$ = 17 Hz, 1F, β-CF), −183.30 (dd, $^3J_{FH}$ = 33.8 Hz, 1F, CHF); ^{31}P{^{1}H}NMR (CD_2Cl_2) δ −37.49 (d, $^3J_{PF}$ = 17.8 Hz, PMe$_3$).

The thermodynamic diastereomer: ^{1}H NMR (CD_2Cl_2) δ 6.75 (ddd, $^2J_{FH}$ = 47.0 Hz, $^3J_{FH}$ = 38.5 Hz, $^3J_{PH}$ = 3.0 Hz, 1H, CHF), 1.95 (dd, $^4J_{PH}$ = 2.0, J = 1.0 Hz, 15H, C$_5$Me$_5$), 1.66 (dd $^2J_{PH}$ = 10.5, J = 1.0 Hz, 9H, PMe$_3$); ^{19}F NMR (CD_2Cl_2) δ −82.97 (d, $^4J_{FF}$ = 12.9 Hz, 3F, CF$_3$), −111.79 (ddd, $^2J_{FF}$ = 273.3 Hz, $^4J_{FP}$ = 24.5 Hz, $^3J_{FF}$ = 17.4 Hz, 1F, β-CF), −116.24 (ddd, $^2J_{FF}$ = 273.3 Hz, $^3J_{FH}$ = 38.5 Hz, $^3J_{FF}$ = 17.4 Hz, 1F, β-CF), −187.68 (ddq, $^2J_{FH}$= 47.0 Hz, $^3J_{FF}$ = 17.4 Hz, $^3J_{PF}$ = 16.1 Hz, 1F, CHF); ^{31}P{^{1}H}NMR (CD_2Cl_2) δ −41.95 (dd, J = 16.7, 16.1 Hz, PMe$_3$).

Reaction of 7a with 2,6-Lutidinium Tetrakis{3,5-bis(trifluoromethyl)phenyl}borate. The solid reagents were weighed into a J-Young NMR tube in the drybox and CD_2Cl_2 (0.5 mL) added by syringe. An immediate color change to yellow was observed. The ^{1}H NMR spectrum (after 10 min) indicated the reaction was complete, with apparent formation of [Cp*Ir(PMe$_3$)(CHFC$_2$F$_5$)]$^+$[B{3,5-C$_6$H$_3$-(CF$_3$)$_2$}$_4$]$^-$. ^{1}H NMR (CD_2Cl_2): δ 8.06 (t, J = 8.1 Hz, 1H, *p*-py-H), 7.78 (br s, 8H, B−(*o*-Ar-*H*), 7.62 (br s, 4H, B−(*p*-Ar-*H*), 7.42 (d, J = 8.1 Hz, 1H, *o*-py-H), 6.82 (dd, J = 44.4, 40.8 Hz, 1H, C*H*F), 2.70 (s, 6H, py*Me*), 1.72 (d, J = 2.1 Hz, 15H, C$_5$*Me*$_5$), 1.58 (d, J = 10.8 Hz, 9H, P*Me*$_3$). ^{19}F NMR (CD_2Cl_2): δ −63.26 (s, B−Ar−C*F*$_3$), −83.25 (s, C*F*$_3$), −112.64 (br d, J = 289.3 Hz, β-C*F*$_2$), −116.53 (br d, J = 289.3 Hz, β-C*F*$_2$), −193.05 (br m, C*H*F). ^{31}P NMR (CD_2Cl_2): δ −24.37 (br m, PMe$_3$). After 30 min, some **6a** was observed by NMR, indicating chloride abstraction from solvent.

General Procedure for NMR Kinetic Experiments. All solid reagents were weighed into a J-Young NMR tube in the drybox. For low-temperature reactions, the sealed tube was then taken out of the box and opened in a liquid nitrogen-cooled Schlenk flask under inert atmosphere. Precooled NMR solvent (0.5−0.6 mL) was then added by syringe and the mixture maintained at low temperature until injection into the NMR probe. For reactions at room temperature or above, the NMR solvent was added in the drybox. An internal integration standard of 1,3,5-trimethoxybenzene was used. Concentration versus time plots were simulated using the IBM chemical kinetics simulator.[84]

Acknowledgment. R.P.H is grateful to the National Science Foundation for generous financial support and to Professors Seth Brown (University of Notre Dame), Chuck Casey (University of Wisconsin, Madison), and Robert Ditchfield (Dartmouth College) for extremely helpful discussions.

JA0545012